Improving qBOLD based measures of oxygen extraction fraction using hyperoxia-BOLD derived measures of blood volume

Alan J Stone[1,2,3], Nicholas P Blockley[1,4]

[1] Wellcome Centre for Integrative Neuroimaging, FMRIB, Nuffield Department of Clinical Neurosciences, University of Oxford, Oxford, United Kingdom

[2] Trinity Centre for Biomedical Engineering, Trinity Biomedical Sciences Institute, Trinity College Dublin, Ireland

[3] Department of Mechanical and Manufacturing Engineering, School of Engineering, Trinity College Dublin, Ireland

[4]School of Life Sciences, University of Nottingham, United Kingdom

Running title: Improving qBOLD measures of OEF using hyperoxia-BOLD

Word count: 5711

Figures: 5 Figures and 2 Tables

References: 44

Address for correspondence: Department of Mechanical & Manufacturing Engineering, Parsons Building, Trinity College Dublin, Dublin 2, Ireland

E-mail address: Alan.Stone@tcd.ie

Abstract

Streamlined-qBOLD (sqBOLD) is a recently proposed refinement of the quantitative BOLD (qBOLD) technique capable of producing non-invasive and quantitative maps of oxygen extraction fraction (OEF) in a clinically feasible scan time. However, sqBOLD measurements of OEF have been reported as being systematically lower than expected in healthy brain. Since the qBOLD framework infers OEF from the ratio of the reversible transverse relaxation rate (R_2') and deoxygenated blood volume (DBV), this underestimation of OEF has been largely attributed to an overestimation of DBV made using this technique.

This study proposes a novel method, hyperoxia-constrained qBOLD (hqBOLD), to improve sqBOLD estimates of OEF. This method circumvents difficulties associated with inferring DBV from the qBOLD model by replacing it with a separate measurement of blood volume derived from hyperoxia-BOLD contrast. In a group of ten healthy volunteers, hqBOLD produced measurements of OEF in cortical grey matter (OEF_{hqBOLD} = 44.7 ± 11.9 %) that were in better agreement with global oximetry measures (OEF_{TRUST} = 40.4 ± 7.7 %), compared to sqBOLD derived measures (OEF_{sqBOLD} = 13.1 ± 4.0 %).

However, in the same group hqBOLD measures of OEF were found to be outside the physiological range in white matter regions (> 100%). By deriving maps of simulated R_2' from TRUST and hyperoxia-BOLD imaging data, the hqBOLD overestimation of OEF in white matter was hypothesised to originate from additional

sources of magnetic susceptibility beyond deoxyhaemoglobin that are present in white matter.

Introduction:

Oxygen extraction fraction (OEF) is an important indicator of the metabolic function of brain tissue that describes the fraction of oxygen removed from arterial blood to serve oxidative metabolism. Imaging methods capable of providing non-invasive parametric maps of OEF can provide key regional information that allows the metabolic profile of brain tissue to be characterised, having applications in the investigation of brain function and disease. Streamlined-quantitative BOLD (sqBOLD) (Stone and Blockley, 2017) is a recently proposed refinement of the quantitative BOLD (qBOLD) (An and Lin, 2003; He and Yablonskiy, 2007; Yablonskiy et al., 2013) technique capable of noninvasively and quantitatively mapping OEF on a regional level. This technique has been shown to be clinically relevant (Stone et al., 2019a), producing parametric maps of tissue oxygenation in clinically appropriate scan times.

DBV overestimation

However, the measurements of OEF made using sqBOLD have been observed to be lower than expected compared to generally accepted literature values (OEF_{sqBOLD} ~ 20%, $OEF_{literature}$ ~ 30 - 40%) (Stone and Blockley, 2017). This underestimation in OEF has largely been attributed to a systematic overestimation in the sqBOLD measurement of deoxygenated blood volume (DBV). There are several potential confounds in the sqBOLD measurement of DBV, including signal from intravascular blood (An and Lin, 2003), diffusion narrowing effects (Dickson et al., 2010; Pannetier et al., 2014; Stone et al., 2019b) and signal from macro-molecules (He and Yablonskiy, 2007). Regardless of the cause of overestimation in DBV, improvements

in the measurement of OEF using sqBOLD can be made by improving the accuracy of DBV.

Independent measure of DBV

One potential solution to this problem is to replace the qBOLD estimate of DBV with a separate independent measure of DBV, an idea originally introduced in the multi-parametric-qBOLD (mp-qBOLD) approach (Christen et al., 2012). The standard qBOLD model describes the transverse MR signal decay in the presence of a network of randomly oriented vessels containing deoxygenated blood. This provides a framework for extracting physiologically relevant measures of DBV and OEF from R_2', the reversible transverse relaxation rate. The qBOLD model describes an additional attenuation at short refocusing offset times that is dependent on the local deoxygenated blood volume (DBV) (Yablonskiy, 1998). With information regarding DBV provided by the mismatch in signal between the mono-exponential and quadratic regimes of the model, a measure related to local vascular oxygenation, such as OEF, can be made by looking at the scaled ratio of R_2' to DBV. The mp-qBOLD approach favours using gadolinium-based dynamic susceptibility contrast (DSC) to provide an independent measure of blood volume and produce quantitative measurements of oxygenation (Christen et al., 2012). The qBOLD based measure of DBV, inferred from the transverse signal decay, is replaced by the DSC measure of cerebral blood volume (CBV) which is combined with a separate measurement of R_2' to estimate OEF. However, DBV in the qBOLD model explicitly refers to the proportion of CBV that contains deoxyhaemoglobin. As such, there is a mismatch between CBV from DSC, which is sensitive to all vessel types and can be

considered a measure of total blood volume, and DBV, which is localised to vessels containing deoxygenated blood such as veins and the pre-venous part of the capillaries (Yablonskiy et al., 2013).

Hyperoxia BOLD

One alternative to DSC based measurements of CBV is to use hyperoxia-BOLD contrast to measure venous CBV (CBV_v). It has been shown that the fractional change in the BOLD signal in response to the administration of oxygen is specific to CBV_v and can be scaled to provide quantitative estimates using a heuristic model (Blockley et al., 2013). The hyperoxia-BOLD and qBOLD techniques rely on the same BOLD contrast. The former uses oxygen as a contrast agent by manipulating the concentration of deoxyhaemoglobin in the deoxygenated blood vessels, whilst the latter relies on the additional signal attenuation due to deoxyhaemoglobin at short refocussing offset times. Therefore, theoretically the CBV_v from hyperoxia-BOLD is equivalent to DBV from qBOLD and henceforth we will refer to both as DBV. In practice hyperoxia-BOLD based measurements are also insensitive to additional sources of magnetic susceptibility beyond deoxyhaemoglobin.

Additional sources of magnetic susceptibility

The original sqBOLD implementation sought to minimise the influence of several confounding effects (cerebral spinal fluid (CSF), irreversible transverse signal decay (T_2) and macroscopic field inhomogeneity) to improve confidence that the measured signal was indeed localised to blood. However, a considerable assumption remains in the qBOLD model that the reversible transverse dephasing (related to R_2') is

exclusively driven by the magnetic susceptibility of deoxyhaemoglobin. In reality, dephasing may also be driven by several non-blood sources of magnetic susceptibility present in the brain. This is particularly relevant in white matter (WM) where the reliability of qBOLD measurements have recently been called into question (Kaczmarz et al., 2019). Axons, within WM fibre bundles, are wrapped in myelin, which is known to possess strong diamagnetic susceptibility (Wharton and Bowtell, 2012). This results in additional dephasing and signal decay that is not accounted for in the qBOLD model. Previous measurements with sqBOLD have found little contrast between GM and WM for both OEF and DBV maps. This is expected for the former, where OEF is expected to be fairly constant across the brain, but, for the latter, DBV is expected to be between 1.7 and 3 times lower in WM compared to GM (Blockley et al., 2013). An independent measure of DBV will enable the effect of additional sources of magnetic susceptibility on estimates of OEF to be investigated.

Study aims

The primary aim of this study is to incorporate an independent and relevant measure of blood volume into the qBOLD framework to offer parametric maps of OEF with improved accuracy compared to sqBOLD. Parametric maps of R_2' are produced using an sqBOLD acquisition and combined with measurements of blood volume made using hyperoxia-BOLD contrast. This multi-parametric approach to measuring and mapping oxygenation is referred to as hyperoxia-constrained qBOLD (hqBOLD). To assess this approach, parametric maps of oxygenation produced using hqBOLD are compared with equivalent maps produced using sqBOLD and whole brain

oximetry measurements of venous oxygenation (TRUST). Whilst hqBOLD is shown to improve estimates of OEF in grey matter, the more robust estimate of blood volume provided by hyperoxia-BOLD contrast highlights the problems with estimating OEF in white matter that are common to sqBOLD. Therefore, the secondary aim of this study is to explore the effects that confound the estimation of OEF in white matter.

Methods

Imaging

Ten healthy participants (aged 23 – 41; median 29; 3 female, 7 male) were scanned with local ethics committee approval using a 3T Siemens Prisma system (Siemens Healthcare, Erlangen, Germany) with a 32-channel receive coil. **Figure 1** presents an overview of the imaging data acquired, the parameters derived from this imaging data and the main comparisons performed in this study. MRI data were acquired in the following order:

TRUST

TRUST oximetry measurements were made in the superior sagittal sinus (SSS) using the following acquisition and labelling parameters: FOV = 230 mm^2, 64 x 64 matrix, repetition time (TR) = 3s, echo time (TE) = 7 ms, GRAPPA = 3, partial Fourier = 6/8, bandwidth = 2604 Hz/px, tag-gap = 25 mm, tag-thickness = 100 mm, inversion-time (TI) = 1050 ms. Four tag–control pairs were acquired at four different effective echo times (eTE = 0, 40, 80 and 160 ms) resulting in thirty-two acquisitions and a total scan duration of 1 minute 53 seconds.

sqBOLD

A conventional qBOLD approach was performed using a FLAIR-GASE acquisition (Blockley and Stone, 2016; Hajnal et al., 1992) acquired with the following parameters: FOV = 220 mm^2, 96 x 96 matrix, nine 5 mm slabs (encoded into four 1.25mm slices, 100% partition oversampling), 2.5 mm gap, TR / TE = 3 s / 80 ms, bandwidth = 2004 Hz/px, TI_{FLAIR} = 1210 ms. Asymmetric spin echo (ASE) with

multiple spin echo displacement times, τ, were acquired at τ = 0 ms (spin-echo, 12 averages) and τ = 15 – 66 ms in steps of 3 ms. This resulted in twenty nine τ-weighted acquisitions with a total scan duration of 12 minutes.

hqBOLD

The data for the hqBOLD approach was collected using two discrete acquisitions to separately measure R_2' and DBV. To provide an independent measure of R_2', the FLAIR-GASE acquisition was repeated for the echo displacement times in the mono-exponential part of the signal decay (τ = 15 – 66 ms in steps of 3 ms) with positioning and all other acquisition parameters being consistent with the sqBOLD acquisition. In a separate acquisition, BOLD-EPI data were acquired with a matched slice prescription to the FLAIR-GASE acquisitions (FOV = 220 mm^2, 96 x 96 matrix, nine 5 mm slices, 2.5 mm gap, TR / TE = 1 s / 35 ms, bandwidth = 2004 Hz/px). A prospective end-tidal gas targeting system (RespirAct™ Gen 3, Thornhill Research Inc., Toronto Canada) was used to modulate end-tidal oxygen ($P_{ET}O_2$) between normoxic and hyperoxic (baseline + 300 mmHg) conditions, whilst maintaining isocapnia (constant CO_2). The hyperoxia paradigm lasted 10 minutes during which time 600 volumes were acquired. The respiratory paradigm consisted of three 2 minute blocks of normoxia interleaved with two 2 minute blocks of hyperoxia (Normoxia (2 min) – Hyperoxia (2 min) – Normoxia (2 min) – Hyperoxia (2 min) – Normoxia (2 min)). To approximately match the total acquisition time of hqBOLD with sqBOLD described above, only the first 5 minutes of the hyperoxia-BOLD data were used in the analysis. Therefore, total acquisition time for hqBOLD was 12 minutes 12

seconds with 7 minutes 12 seconds being used for the R_2' measurement and 5 minutes being used for the hyperoxia-BOLD measurement of volume.

A high-resolution T_1-weighted structural image (FOV = 174 mm x 192 mm x 192 mm, 116 x 128 x 128 matrix, TR / TI / TE = 1900 / 904 / 3.74 ms and flip angle 8°) was acquired in each subject. (Mugler and Brookeman, 1990). To aid in the registration of the FLAIR-GASE to the structural image, an additional set of whole brain GASE data without a FLAIR preparation was acquired with an increased coverage in the z direction (FOV = 220 mm^2, 96 x 96 matrix, twenty four 5 mm slices, 2.5 mm gap, TR / TE = 1 s / 35 ms, bandwidth = 2004 Hz/px).

Data Analysis

The following pre-processing and analysis steps were performed to the data acquired in each subject using a combination of tools from the FMRIB Software Library (FSL) (Jenkinson et al., 2012) and custom scripts written using MATLAB (The Mathworks, Natick, MA).

TRUST

Tag-control images were first motion corrected using the FMRIB FSL linear motion correction tool (MCFLIRT) (Jenkinson et al., 2002). Pairwise subtraction of the tag-control images was performed and the four repeats at each eTE averaged. Using the difference image at eTE = 0 ms, the four voxels with the highest signal in the SSS were identified using an automated registration and masking routine to create a region of interest (ROI). Using the SSS ROI, the mean difference signal (ΔS) was

extracted for each eTE. To calculate the T_2 of blood (T_{2b}), ΔS is plotted as a function of eTE and fitted to Equation 1 to obtain the exponent C (Lu and Ge, 2008).

$$\Delta S = S_0 e^{eTE.C} \qquad \textbf{Eqn. 1}$$

T_{2b} was then estimated from C using Equation 2 (Lu et al., 2004) and assuming the T_1 of blood (T_{1b}) to be 1624 ms.

$$T_{2b} = \frac{1}{\frac{1}{T_{1b}} - C} \qquad \textbf{Eqn. 2}$$

Assuming a value for haematocrit in large vessels (Hct = 0.42 (Peng et al., 2014)), T_{2b} can be converted to venous blood oxygenation (Y_v) based on a known relationship between oxygenation and T_{2b} (Lu et al., 2012). Assuming arterial blood is fully saturated, an estimate of whole brain OEF is given by 1-Y_v.

sqBOLD

The four 1.25 mm slices of each slab of the FLAIR-GASE data were averaged to produce nine 5 mm slices. The sqBOLD and hqBOLD τ-series were concatenated together and motion corrected using MCFLIRT (Jenkinson et al., 2002). The temporal mean of this concatenated data set was brain extracted using the FSL brain extraction tool (BET) (Smith, 2002) to create a binary mask of brain tissue and further analysis was restricted to voxels within this mask. The sqBOLD τ-series for each voxel were then fit using a linear system (A · x = B) to simultaneously estimate

R_2', DBV and a constant term representing the underlying proton density and T_2 decay (Stone et al., 2019a).

$$\begin{bmatrix} 0 & 0 & 1 \\ 0 & 0 & 1 \\ \vdots & \vdots & \vdots \\ 1 & -\tau_1 & 1 \\ 1 & -\tau_2 & 1 \\ \vdots & \vdots & \vdots \\ 1 & -\tau_n & 1 \end{bmatrix} \begin{bmatrix} DBV \\ R_2' \\ \log(S_0) - TE \cdot R_2 \end{bmatrix} = \begin{bmatrix} \log(S(\tau_0)) \\ \log(S(\tau_0)) \\ \vdots \\ \log(S(\tau_1)) \\ \log(S(\tau_2)) \\ \vdots \\ \log(S(\tau_n)) \end{bmatrix} \qquad \textbf{Eqn. 3}$$

Here, S(τ) is the signal intensity as a function of τ, where τ_0 represents the multiple τ = 0 ms acquisitions and τ_1 to τ_n are values of τ > 15 ms. In matrix A the first two rows describe the short τ regime relevant to τ_0 and subsequent rows the long τ regime representing τ > 15 ms (Yablonskiy and Haacke, 1994). The least squares solution was used to produce voxel-wise estimates of R_2' and DBV. Parameter maps of OEF were then calculated using Equation 4 with known or assumed constants for the susceptibility difference between oxygenated and deoxygenated red blood cells ($\Delta\chi_0 = 0.264 \times 10^{-6}$ (Spees et al., 2001)) and haematocrit in small vessels (Hct = 0.34 (Eichling et al., 1975)).

$$OEF = \frac{R_2'}{DBV \cdot \gamma \cdot \frac{4}{3} \cdot \pi \cdot \Delta\chi_0 \cdot Hct \cdot B_0} \qquad \textbf{Eqn. 4}$$

hqBOLD

For the multi-parametric hqBOLD approach, an independent parameter map of R_2' was calculated from the hqBOLD τ-series using a log-linear least squares fit in the

long τ regime only for R_2' and the constant term. The hyperoxia-BOLD data were then analysed in the following way. The BOLD data were motion corrected using MCFLIRT. The temporal mean was used to align this data with temporal mean of the concatenated FLAIR-GASE data using FLIRT and the BOLD data were then transformed into the FLAIR-GASE image space using *applywarp* (Jenkinson and Smith, 2001). Measurements of end-tidal partial pressure of oxygen ($P_{ET}O_2$) were manually checked for accuracy and interpolated onto the 1 sec time resolution of the BOLD data. This $P_{ET}O_2$ time-course was then smoothed to generate a regressor representing the *in vivo* time-course of blood oxygenation change. When combined with a constant term, this model was fitted to the hyperoxia-BOLD data on a voxel-wise basis using the least squares method to yield the change in signal and the baseline signal. The ratio of these parameters was then used to calculate the fractional BOLD signal change in response to the hyperoxia challenge (δS). The change in $P_{ET}O_2$ during the hyperoxia challenge ($\Delta P_{ET}O_2$) was calculated by taking the mean of data within windows during baseline (repetitions 1 to 100) and hyperoxia (repetitions 175 to 225). These measurements were used to calculate DBV, under the assumption that $\Delta P_{ET}O_2 = \Delta P_aO_2$ (the change in arterial partial pressure of oxygen) using Equation 5, where A = 27 ms, B = 0.2, C = 245.1 mmHg, D = 0.1.

$$DBV = \left(\frac{A}{TE} + B\right)\left(\frac{C}{\Delta P_a O_2} + D\right)\delta S \qquad \textbf{Eqn. 5}$$

Investigating additional contributions to the reversible transverse relaxation rate

Empirical physiological measurements of OEF and DBV that are unconfounded by additional sources of magnetic susceptibility can be used to simulate estimates of R_2' ($R_2'_{sim}$) in the absence of such sources (Equation 4).

$$R_2'_{sim} = \gamma \cdot \frac{4}{3} \cdot \pi \cdot \Delta\chi_0 \cdot Hct \cdot B_0 \cdot OEF \cdot DBV \qquad \textbf{Eqn. 6}$$

In this study, OEF was measured using the TRUST technique and DBV using the hyperoxia-BOLD based method. These techniques were chosen to minimise sensitivity to additional sources of magnetic susceptibility. Maps of $R_2'_{sim}$ were calculated for each participant from the voxel-wise measures of DBV from the hyperoxia-BOLD maps and assuming a single value of OEF across the whole brain from the TRUST measurement. As such, this approach assumes that OEF is regionally uniform across the healthy, resting brain.

For comparison, R_2' was measured ($R_2'_{meas}$) using the FLAIR-GASE acquisition using the data acquired for hqBOLD. These measurements are considered to contain contributions to $R_2'_{meas}$ from both deoxyhaemoglobin and non-deoxyhaemoglobin origins. Consistency between $R_2'_{sim}$ and $R_2'_{meas}$ would suggest a small contribution of these additional (non-deoxyhaemoglobin) sources to the measured sqBOLD signal, whereas a large mismatch would suggest sqBOLD oxygenation measurements are substantially confounded by other (non-deoxyhaemoglobin) sources of magnetic susceptibility.

Regional Analysis

Subject specific ROIs of cortical grey matter (GM) and white matter (WM) were created. Typically, a high resolution T_1-weighted structural image is segmented into three components; GM, WM and CSF. However, GM ROI estimates were found to be particularly sensitive to accurate registration between the FLAIR-GASE/BOLD data with matched EPI bandwidth and the T_1-weighted structural. This was particularly evident in the mapping of sulci between these modalities. However, T_1-weighting in the FLAIR-GASE was sufficient to enable a good segmentation of the temporal mean of the concatenated FLAIR-GASE data using FAST (Zhang et al., 2001). GM partial volume estimate (PVE) maps were threshold at 50% and further refined to cortical GM by transforming the MNI structural atlas (Mazziotta et al., 2001) into the FLAIR-GASE space. This was achieved by registering the MNI brain template to the concatenated FLAIR-GASE reference, firstly, via the whole brain GASE data and, secondly, via the T_1-weighted structural using FLIRT. Only the frontal, insula, occipital, parietal and temporal lobes were included in the cortical mask to produce the final cortical GM ROI. WM ROIs were generated by thresholding the WM PVE maps at 100%.

Statistical testing

A one-way ANOVA was used to test the null hypothesis of no difference between the OEF estimates made using the three different techniques (**Table 1**). Post-hoc statistical testing was performed using the Tukey Kramer method (honest significant difference test) to test for differences between the estimates made using the different methods. A paired t-test was used to test the null hypothesis of no difference

between the DBV estimates made using sqBOLD and hyperoxia-BOLD (**Table 1**). The coefficient-of-variation (CoV) across the group was calculated for each of the estimates by dividing the group standard deviation by the group mean (**Table 1**). A one-way ANOVA was used to test the null hypothesis of no difference between $R_2'_{meas}$ and $R_2'_{sim}$ measures in grey and white matter (**Table 2**). Post-hoc statistical testing was performed using the Tukey Kramer method (honest significant difference test) to test for differences between the measures of R_2'.

Results

Figure 2 shows parameter maps of DBV and OEF made using hqBOLD (column one and two) and sqBOLD (column three and four). These parameter maps show a single slice from each of the ten subjects imaged in the study. On initial inspection the DBV maps produced using hyperoxia-BOLD demonstrate an obvious contrast between grey and white matter with white matter values being consistently lower. The hqBOLD OEF maps show grey matter values that are within the physiologically plausible range for healthy brain tissue. In comparison, the sqBOLD derived DBV and OEF parameter maps demonstrate little contrast between grey and white matter, agreeing well with the initial implementation of this method (Stone and Blockley, 2017). It should be noted that a threshold was applied to the hqBOLD OEF maps, displayed in **Figure 2**, to exclude values outside the physiologically plausible range (0 - 100%). Estimates of OEF in white matter fall outside this range (>100%). The reliability of qBOLD measurements in white matter are investigated later in this section.

Table 1 shows regional estimates in grey matter extracted from hqBOLD and sqBOLD parameter maps for the group of healthy volunteers. These estimates are compared to values of global OEF measured using TRUST. In grey matter, hyperoxia-BOLD derived DBV was significantly different to sqBOLD derived DBV across the group ($p < 0.05$, group average: $DBV_{hqBOLD} = 1.6 \pm 0.6$ %; $DBV_{sqBOLD} = 3.7 \pm 1.7$ %). The grey matter OEF values measured across the group differed significantly between the three different techniques (One-way ANOVA, $p < 0.001$). Post-hoc pairwise comparisons of the grey matter OEF measured with each

method revealed that OEF_{sqBOLD} is significantly different to OEF_{hqBOLD} ($p < 0.0001$) and OEF_{TRUST} ($p < 0.0001$), but that there was no significant difference between OEF_{hqBOLD} and OEF_{TRUST} ($p = 0.51$). The estimates of OEF in grey matter show a similar CoV across the three techniques ($CoV_{hqBOLD} = 0.27$; $CoV_{TRUST} = 0.19$; $CoV_{sqBOLD} = 0.30$), but with the qBOLD methods providing additional regional information not available using TRUST.

Figure 3 shows histograms of DBV_{hqBOLD} (**Figure 3a**), OEF_{hqBOLD} (**Figure 3b**), DBV_{sqBOLD} (**Figure 3c**) and OEF_{sqBOLD} (**Figure 3d**) voxel values contained within grey matter for each of the ten healthy subjects. These histograms show the distribution of voxel values that underlie the measurements presented in **Table 1**. Histograms of DBV_{hqBOLD} exhibit narrower distributions of voxel values compared to DBV_{sqBOLD} distributions. For each subject, histograms of OEF_{hqBOLD} exhibit a higher median OEF (**Figure 3**, red-line) in each subject with a broader distribution of values compared to OEF_{sqBOLD}.

Figure 4 shows grey matter OEF_{TRUST} compared to OEF_{hqBOLD} (**Figure 4a**) and OEF_{sqBOLD} (**Figure 4b**). Bland-Altman plots demonstrate a large bias between OEF_{TRUST} and OEF_{sqBOLD} of -27.3 percentage points whereas OEF_{TRUST} and OEF_{hqBOLD} are in better agreement with a smaller bias of +4.2 points between techniques.

Figure 5 shows a comparison between measured ($R_2'_{meas}$) and simulated ($R_2'_{sim}$) maps of R_2' for nine slices in an example subject. Differences are apparent between these maps with $R_2'_{sim}$ demonstrating high R_2' in the regions of grey matter and low R_2' in regions of white matter, whilst $R_2'_{meas}$ exhibits high regional R_2' in both grey and white matter regions.

Table 2 displays regional estimates of $R_2'_{meas}$ and $R_2'_{sim}$ in grey and white matter for the group of healthy volunteers. A significant difference between regional measurements of R_2' was found (One-way ANOVA, $p < 0.001$). Post-hoc pairwise comparisons in grey matter showed $R_2'_{meas}$ is significantly different to $R_2'_{sim}$ ($p < 0.05$) and was also significantly different to white matter parameters ($R_2'_{meas}$ ($p < 0.01$) and $R_2'_{sim}$ ($p < 0.0001$)). Comparing the measurements made in white matter, $R_2'_{meas}$ was measured to be significantly higher than $R_2'_{sim}$ ($p < 0.0001$). This suggests a considerable non-blood contribution to the measured signal ($R_2'_{meas}$) in white matter.

Discussion

In this study we investigated a novel technique that incorporates an independent measure of blood volume into the qBOLD framework to provide parametric maps of OEF with improved accuracy compared to sqBOLD. To calculate parametric maps of OEF, this technique, referred to here as hyperoxia-constrained qBOLD or hqBOLD, combines relaxometry based measures of reversible transverse relaxation rate (R_2') with regional estimates of DBV made using hyperoxia-BOLD. Through combining hyperoxia-BOLD derived parametric maps of DBV with asymmetric spin echo derived parameter maps of R_2', the measures of OEF derived from hqBOLD (range 27 – 58 %) are shown to agree well with literature values of OEF in healthy cortical grey matter (~ 35 - 55 %) (Marchal et al., 1992), in comparison to sqBOLD derived measures of OEF which are considered to be systematically low (range 7 – 19 %) (**Table 1**). Furthermore, grey matter measures of OEF_{hqBOLD} are in better agreement with global cerebral oxygenation measurements made with TRUST oximetry (range 28 – 53 %). Although hqBOLD is shown to improve estimates of OEF in grey matter, estimates of OEF in white matter are outside of the physiological range (OEF > 100 %). Comparison of measurements of R_2' with simulation of the expected R_2' due to deoxyhaemoglobin alone, suggests that the overestimation of OEF measured in white matter may be due to additional sources of magnetic susceptibility.

Grey matter

Across the group, measurements of blood volume in healthy cortical grey matter made using hyperoxia-BOLD (range DBV = 1.1 – 2.8 %) demonstrate less variability compared to the sqBOLD derived measurements (range DBV = 1.6 – 6.9 %) (**Table**

1). The range of the latter is somewhat broader than previously observed using the same technique (range DBV_{sqBOLD} = 3.0 – 4.4 % (Stone and Blockley, 2017)), whilst the former is in reasonable agreement with past measurements (range DBV_{hqBOLD} = 1.8 – 2.8 % (Blockley et al., 2013)). Grey matter DBV measured using hqBOLD was found to be significantly different to sqBOLD derived DBV ($p < 0.05$), with DBV_{sqBOLD} 2.3 times higher than DBV_{hqBOLD} on average. As previously mentioned, the qBOLD framework uses the ratio of R_2' to DBV to calculate parametric maps of OEF (**Equation 4**) and replacing the elevated sqBOLD DBV measurement with the hyperoxia-BOLD DBV yields a significant difference ($p < 0.0001$) in the final calculated values of OEF that are better aligned with a well validated whole brain measurement of OEF (TRUST). **Equation 4** predicts that OEF should increase in proportion to the decrease in DBV. However, on average OEF_{hqBOLD} is 3.4 times greater than OEF_{sqBOLD} (rather than 2.4 times predicted from the reduced DBV). This may be explained by the clear differences in the distributions of DBV_{sqBOLD} and DBV_{hqBOLD} voxel values (**Figure 3**), resulting in the individual medians being elevated to a greater degree than predicted.

Validation

The Kety-Schmidt method allows the OEF of the whole brain to be measured with minimal assumptions (Kety and Schmidt, 1948). This is achieved by extracting arterial blood from the brachial or femoral arteries and venous blood from the jugular bulb. This procedure is invasive and rarely practical for the validation of newly developed MRI techniques. One alternative is the T2-relaxation-under-spin-tagging (TRUST) technique. TRUST is a widely used, MR based method for inferring blood

oxygenation levels that has been thoroughly optimised (Lu et al., 2012; Xu et al., 2012) and tested (Jiang et al., 2018). As such, TRUST presents a quick, convenient and robust global measurement against which to benchmark the development of new methods for mapping brain oxygenation.

Bland-Altman plots demonstrate that measurements of grey matter OEF made with hqBOLD agree well with TRUST oximetry across the group (**Figure 4a**). The bias between the two methods is acceptable for the cohort imaged in this study ($\left|\mathrm{OEF}_{\mathrm{hqBOLD}} - \mathrm{OEF}_{\mathrm{TRUST}}\right| = 4.2\%$) and all individual differences lie within the 95% limits of agreement. In contrast, sqBOLD measures of OEF in grey matter demonstrate poor agreement and a large bias when compared to TRUST oximetry ($\left|\mathrm{OEF}_{\mathrm{sqBOLD}} - \mathrm{OEF}_{\mathrm{TRUST}}\right| = 27.3\%$) (**Figure 4b**).

White matter

Parameter maps of OEF produced using the hqBOLD approach demonstrate physiologically unrealistic values (> 100%) in regions of white matter (**Figure 2**). This is likely due to the presence of an additional source of magnetic susceptibility from white matter, which is not accounted for in the qBOLD model. By combining measures of DBV from hyperoxia-BOLD and whole brain OEF from TRUST, simulated maps of R_2' can be calculated ($R_2'_{sim}$ cf. **Equation 6**) for each subject. In contrast, the ASE based measure of R_2', that forms the basis of the qBOLD approaches presented in this paper, can be considered to have magnetic susceptibility contributions from deoxyhaemoglobin and additional sources, and as

such these maps are referred to as $R_2'_{meas}$. For successful implementation of the qBOLD model, measured R_2' is assumed to only include signal that originates from deoxyhaemoglobin. However, unless contributions from additional sources of magnetic susceptibility are explicitly removed or minimised by the acquisition, the application of the existing qBOLD model will yield confounded estimates of oxygenation. Additionally, the FLAIR-GASE acquisition explicitly removes the confounding effect of CSF, macroscopic magnetic field inhomogeneity and T_2, but additional confounding signals not explicitly accounted for could result in the misestimation of OEF.

Differences in regional contrast between $R_2'_{meas}$ (**Figure 5a**) and $R_2'_{sim}$ (**Figure 5b**) are clearly evident in the calculated parameter maps, with significant differences between $R_2'_{meas}$ and $R_2'_{sim}$ in both grey matter ($p < 0.05$) and white matter ($p < 0.0001$) (**Table 2**). However, the magnitude of this difference varies with $R_2'_{meas}$ 1.5 times greater than $R_2'_{sim}$ in grey matter and 6.5 times greater in white matter. These results suggest that a large additional magnetic susceptibility contribution is present in white matter. Whilst in grey matter this variation could be accounted for in the constants that describe **Equation 6** or by partial volume incorporated in the grey matter ROI.

One obvious source, that potentially accounts for the larger discrepancy between $R_2'_{sim}$ and $R_2'_{meas}$ in white matter compared to grey matter, is myelin. The high

myelin content of white matter (compared to its relative sparsity in grey matter) has previously been suggested as a confounding factor for qBOLD based measures of oxygenation in white matter (Bouvier et al., 2013). Myelin is the lipid rich insulating layer that surrounds axons and has been shown to have its own distinct susceptibility characteristics that would significantly contribute towards $R_2'_{meas}$ in white matter (Hirsch et al., 2014). As the qBOLD model assumes that the ASE signal is localised to deoxyhaemoglobin, the additional signal contribution of myelin is not accounted for in the qBOLD model and will lead to error in the final oxygenation parameter estimates. This has previously been shown to have an influence on the estimates of OEF and DBV made using mp-qBOLD (Kaczmarz et al., 2019).

Comparison with alternative techniques

The hqBOLD method, as presented in its current state, requires further refinement for clinical implementation in acutely ill patients due to relatively long scan-times, use of respiratory manipulations and confounded white matter measures. However, this approach does compare well with similar MRI based methods such as mp-qBOLD and dual-calibrated FMRI and is suitable in its current form for research applications and certain clinical applications that don't include acutely ill patients.

The total acquisition time for the hqBOLD approach was 12 mins 12 secs. This is marginally greater than the acquisition time for mp-qBOLD (~10 minutes) and shorter than the acquisition time used for dual calibrated FMRI (Bulte et al., 2012; Gauthier et al., 2012; Wise et al., 2013). However, the total acquisition time of the hqBOLD

approach implemented here was not optimised and there is considerable scope for shortening the FLAIR-GASE and hyperoxia-BOLD components of the acquisition.

In terms of external contrast agents, the mp-qBOLD method uses gadolinium contrast agent to provide an independent measure of blood volume whereas dual-calibrated FMRI uses a combination of hyperoxic and hypercapnic respiratory challenges to produce maps of cerebral oxygenation. Contrasting hqBOLD with mp-qBOLD and dual-calibrated FMRI, the method presented here circumvents the use of gadolinium (mp-qBOLD), avoiding concerns regarding gadolinium use (Gulani et al., 2017), and hypercapnia (dual-calibrated FMRI), with its associated subject comfort and tolerability issues (Chiarelli et al., 2007; Mohtasib et al., 2012). Furthermore, hqBOLD directly measures R_2' using an asymmetric spin echo. This circumvents concerns around noise propagation when calculating R_2' from the subtraction of R_2 from R_2^* as used in mp-qBOLD.

For all three methods, cerebral oxygenation measurements in white matter are unreliable and require further work for different reasons. The hqBOLD and mp-qBOLD methods are limited by non-blood contributions to the R_2' in white matter. Dual-calibrated FMRI is limited by the ability of arterial spin labelling to make meaningful measurements of blood flow in white matter.

Limitations and future work

It is worth noting some of the relevant limitations of the protocols used in this study. The sqBOLD protocol used here has only minor differences compared with previous

studies i.e. an increased number of spin echo averages and slightly denser sampling of long τ values. We have shown that the long TE used here (TE = 80 ms) results in increased signal loss at the spin echo, due to the scale of the vessel distribution approaching the diffusion narrowing regime, causing DBV to be overestimated (Stone et al., 2019b). Unfortunately acquisition of the data in this study commenced before this simulation study had been completed and hence any improvements could not be implemented. Similarly, we have developed a Bayesian analysis tool for sqBOLD data, which has been shown to reduce the variance in parameter estimates (Cherukara et al., 2019). However, since a tool to analyse the hqBOLD data in a Bayesian framework was not available, we chose to use least squares fitting for both techniques. However, we remain hopeful that an optimised sqBOLD protocol coupled with Bayesian model fitting can overcome some of the inaccuracy of the protocol used here.

One particular challenge with hqBOLD is the registration between the two sets of data. Whilst EPI bandwidth was matched to ensure consistent distortion, the image contrast was markedly different between them, with CSF showing as bright in the BOLD images and dark in the GASE data. In future this might be solved by using unsuppressed GASE data with the effect of CSF removed in post-processing or by using a FLAIR-GASE acquisition throughout. However, the biggest challenge to accurate estimates of OEF across the brain is the presence of additional sources of magnetic susceptibility. Further modelling work similar to that used to investigate overestimation of DBV in grey matter will be required (Stone et al., 2019b), which will hopefully provide new avenues to mitigate or correct for these effects.

The TRUST protocol used in this study had a longer echo time (7 ms) than that recommended (3.6 ms). This has been shown to result in an overestimation of $R_{2\,blood}$ (Xu et al., 2012) that leads to a slight overestimation in OEF of approximately 3-4%. However, this overestimation has been shown to be reliant on measurement SNR and as such, the number of averages acquired in this study was increased from the recommended number of three to four. Further to this, the group mean and coefficient of variation for OEF_{TRUST} measured in this study (OEF_{TRUST} = 40.4 %; CoV_{TRUST} = 0.19) is comparable with previous validation of this method (OEF_{TRUST} = 37.5 %; CoV_{TRUST} = 0.16) (Liu et al., 2013). Further limitations of the TRUST based measurement of OEF presented in this study are associated with the assumption of model parameters, arterial blood oxygenation (Y_a) and blood haematocrit level (Hct) (**Equation 2**). Although the inclusion of individual parameter estimates of Y_a and Hct would increase the precision of OEF_{TRUST} in this study, the investigated cohort are young and healthy and inter-individual differences in these parameters are expected to be small.

Conclusion

By combining a relaxometry based measure of R_2' with a hyperoxia-BOLD derived measure of blood volume, hyperoxia-qBOLD demonstrated improved estimates of OEF in cerebral grey matter compared to streamlined-qBOLD. Estimates of OEF in white matter made using this method were found to be outside the physiological range. Further investigation revealed that elevations in white matter OEF were due to a higher measured R_2' compared with the simulated maps of R_2' predicted by the

qBOLD model. This elevated R_2' is hypothesised to be due to additional sources of susceptibility beyond deoxyhaemoglobin. With further refinement this method has the potential to offer a clinically relevant measure of cerebral oxygenation.

Acknowledgements

This work was funded by EPSRC grant EP/K025716/1.

Appendix A. Supplementary data

The raw imaging data that underpins this work can be accessed via the Oxford Research Archive repository, doi: 10.5287/bodleian:X59eGb0pv. In addition, analysis code for this study can be accessed via Zenodo, doi: 10.5281/zenodo.3886937.

References

An, H., Lin, W., 2003. Impact of intravascular signal on quantitative measures of cerebral oxygen extraction and blood volume under normo- and hypercapnic conditions using an asymmetric spin echo approach. Magn. Reson. Med. 50, 708–716. https://doi.org/10.1002/mrm.10576

Berman, A.J.L., Pike, G.B., 2018. Transverse signal decay under the weak field approximation: Theory and validation. Magn. Reson. Med. https://doi.org/10.1002/mrm.27035

Blockley, N.P., Griffeth, V.E.M., Germuska, M.A., Bulte, D.P., Buxton, R.B., 2013. An analysis of the use of hyperoxia for measuring venous cerebral blood volume: Comparison of the existing method with a new analysis approach. Neuroimage 72, 33–40. https://doi.org/10.1016/j.neuroimage.2013.01.039

Blockley, N.P., Stone, A.J., 2016. Improving the specificity of R2' to the deoxyhaemoglobin content of brain tissue: Prospective correction of macroscopic magnetic field gradients. Neuroimage 135, 253–260. https://doi.org/10.1016/j.neuroimage.2016.04.013

Bouvier, J., Castellani, S., Debacker, C., Pannetier, N., Troprès, I., Krainik, A., Barbier, E.L., 2013. Evalutation of multiparametric qBOLD in white matter: a simulation study. Proc. Intl. Soc. Mag. Reson. Med. 21 21, 2942.

Bulte, D.P., Kelly, M., Germuska, M., Xie, J., Chappell, M.A., Okell, T.W., Bright, M.G., Jezzard, P., 2012. Quantitative measurement of cerebral physiology using respiratory-calibrated MRI. Neuroimage. https://doi.org/10.1016/j.neuroimage.2011.12.017

Cherukara, M.T., Stone, A.J., Chappell, M.A., Blockley, N.P., 2019. Model-based

Bayesian inference of brain oxygenation using quantitative BOLD. Neuroimage 202, 116106. https://doi.org/10.1016/j.neuroimage.2019.116106

Chiarelli, P.A., Bulte, D.P., Gallichan, D., Piechnik, S.K., Wise, R., Jezzard, P., 2007. Flow-metabolism coupling in human visual, motor, and supplementary motor areas assessed by magnetic resonance imaging. Magn. Reson. Med. https://doi.org/10.1002/mrm.21171

Christen, T., Schmiedeskamp, H., Straka, M., Bammer, R., Zaharchuk, G., 2012. Measuring brain oxygenation in humans using a multiparametric quantitative blood oxygenation level dependent MRI approach. Magn. Reson. Med. 68, 905–911. https://doi.org/10.1002/mrm.23283

Dickson, J.D., Ash, T.W.J., Williams, G.B., Harding, S.G., Carpenter, T.A., Menon, D.K., Ansorge, R.E., 2010. Quantitative BOLD: the effect of diffusion. J. Magn. Reson. Imaging 32, 953–961. https://doi.org/10.1002/jmri.22151

Eichling, J.O., Raichle, M.E., Grubb, R.L., Larson, K.B., Ter-Pogossian, M.M., 1975. In vivo determination of cerebral blood volume with radioactive oxygen 15 in the monkey. Circ. Res. https://doi.org/10.1161/01.RES.37.6.707

Gauthier, C.J., Desjardins-Crépeau, L., Madjar, C., Bherer, L., Hoge, R.D., 2012. Absolute quantification of resting oxygen metabolism and metabolic reactivity during functional activation using QUO2 MRI. Neuroimage. https://doi.org/10.1016/j.neuroimage.2012.07.065

Gulani, V., Calamante, F., Shellock, F.G., Kanal, E., Reeder, S.B., 2017. Gadolinium deposition in the brain: summary of evidence and recommendations. Lancet Neurol. 16, 564–570. https://doi.org/10.1016/S1474-4422(17)30158-8

Hajnal, J. V., de Coene, B., Lewis, P.D., Baudouin, C.J., Cowan, F.M., Pennock,

J.M., Young, I.R., Bydder, G.M., 1992. High signal regions in normal white matter shown by heavily T2-weighted CSF nulled IR sequences. J. Comput. Assist. Tomogr. 16, 506–513. https://doi.org/10.1097/00004728-199207000-00002

He, X., Yablonskiy, D.A., 2007. Quantitative BOLD: Mapping of human cerebral deoxygenated blood volume and oxygen extraction fraction: Default state. Magn. Reson. Med. 57, 115–126. https://doi.org/10.1002/mrm.21108

Hirsch, N.M., Toth, V., Förschler, A., Kooijman, H., Zimmer, C., Preibisch, C., 2014. Technical considerations on the validity of blood oxygenation level-dependent-based MR assessment of vascular deoxygenation. NMR Biomed. 27, 853–862. https://doi.org/10.1002/nbm.3131

Jenkinson, M., Bannister, P., Brady, M., Smith, S., 2002. Improved optimization for the robust and accurate linear registration and motion correction of brain images. Neuroimage 17, 825–841. https://doi.org/10.1016/S1053-8119(02)91132-8

Jenkinson, M., Beckmann, C.F., Behrens, T.E.J., Woolrich, M.W., Smith, S.M., 2012. FSL. Neuroimage 62, 782–790. https://doi.org/10.1016/j.neuroimage.2011.09.015

Jenkinson, M., Smith, S., 2001. A global optimisation method for robust affine registration of brain images. Med. Image Anal. 5, 143–156. https://doi.org/10.1016/S1361-8415(01)00036-6

Jiang, D., Liu, P., Li, Y., Mao, D., Xu, C., Lu, H., 2018. Cross-vendor harmonization of T2-relaxation-under-spin-tagging (TRUST) MRI for the assessment of cerebral venous oxygenation. Magn. Reson. Med. 80, 1125–1131.

https://doi.org/10.1002/mrm.27080

Kaczmarz, S., Göttler, J., Zimmer, C., Hyder, F., Preibisch, C., 2019. Characterizing white matter fiber orientation effects on multi-parametric quantitative BOLD assessment of oxygen extraction fraction. J. Cereb. Blood Flow Metab. https://doi.org/10.1177/0271678X19839502

Kety, S.S., Schmidt, C.F., 1948. The effects of altered arterial tensions of carbon dioxide and oxygen on cerebral blood flow and cerebral oxygen consumption of normal young men. J. Clin. Invest. https://doi.org/10.1172/JCI101995

Liu, P., Xu, F., Lu, H., 2013. Test-retest reproducibility of a rapid method to measure brain oxygen metabolism. Magn. Reson. Med. 69, 675–681. https://doi.org/10.1002/mrm.24295

Lu, H., Clingman, C., Golay, X., Van Zijl, P.C.M., 2004. Determining the longitudinal relaxation time (T1) of blood at 3.0 tesla. Magn. Reson. Med. 52, 679–682. https://doi.org/10.1002/mrm.20178

Lu, H., Ge, Y., 2008. Quantitative evaluation of oxygenation in venous vessels using T2-relaxation-under-spin-tagging MRI. Magn. Reson. Med. 60, 357–363. https://doi.org/10.1002/mrm.21627

Lu, H., Xu, F., Grgac, K., Liu, P., Qin, Q., Van Zijl, P., 2012. Calibration and validation of TRUST MRI for the estimation of cerebral blood oxygenation. Magn. Reson. Med. 67, 42–49. https://doi.org/10.1002/mrm.22970

Marchal, G., Rioux, P., Sette, G., Derlon, J.M., Baron, J.C., Petit Taboué, M.C., Travère, J.M., Poec, C., Courtheoux, P., 1992. Regional Cerebral Oxygen Consumption, Blood Flow, and Blood Volume in Healthy Human Aging. Arch. Neurol. https://doi.org/10.1001/archneur.1992.00530340029014

Mazziotta, J., Toga, A., Evans, A., Fox, P., Lancaster, J., Zilles, K., Woods, R., Paus, T., Simpson, G., Pike, B., Holmes, C., Collins, L., Thompson, P., MacDonald, D., Iacoboni, M., Schormann, T., Amunts, K., Palomero-Gallagher, N., Geyer, S., Parsons, L., Narr, K., Kabani, N., Le Goualher, G., Boomsma, D., Cannon, T., Kawashima, R., Mazoyer, B., 2001. A probabilistic atlas and reference system for the human brain: International Consortium for Brain Mapping (ICBM). Philos. Trans. R. Soc. B Biol. Sci. 356, 1293–1322. https://doi.org/10.1098/rstb.2001.0915

Mohtasib, R.S., Lumley, G., Goodwin, J.A., Emsley, H.C.A., Sluming, V., Parkes, L.M., 2012. Calibrated fMRI during a cognitive Stroop task reveals reduced metabolic response with increasing age. Neuroimage. https://doi.org/10.1016/j.neuroimage.2011.07.092

Mugler, J.P., Brookeman, J.R., 1990. Three-dimensional magnetization-prepared rapid gradient-echo imaging (3D MP RAGE). Magn. Reson. Med. https://doi.org/10.1002/mrm.1910150117

Pannetier, N.A., Sohlin, M., Christen, T., Schad, L., Schuff, N., 2014. Numerical modeling of susceptibility-related MR signal dephasing with vessel size measurement: phantom validation at 3T. Magn. Reson. Med. 72, 646–658. https://doi.org/10.1002/mrm.24968

Peng, S.L., Dumas, J.A., Park, D.C., Liu, P., Filbey, F.M., McAdams, C.J., Pinkham, A.E., Adinoff, B., Zhang, R., Lu, H., 2014. Age-related increase of resting metabolic rate in the human brain. Neuroimage 98, 176–183. https://doi.org/10.1016/j.neuroimage.2014.04.078

Smith, S.M., 2002. Fast robust automated brain extraction. Hum. Brain Mapp. 17,

143–155.

Spees, W.M., Yablonskiy, D.A., Oswood, M.C., Ackerman, J.J.H., 2001. Water proton MR properties of human blood at 1.5 Tesla: Magnetic susceptibility, T1, T2*, T2, and non-Lorentzian signal behavior. Magn. Reson. Med. https://doi.org/10.1002/mrm.1072

Stone, A.J., Blockley, N.P., 2017. A streamlined acquisition for mapping baseline brain oxygenation using quantitative BOLD. Neuroimage 147, 79–88. https://doi.org/10.1016/j.neuroimage.2016.11.057

Stone, A.J., Harston, G.W.J., Carone, D., Okell, T.W., Kennedy, J., Blockley, N.P., 2019a. Prospects for investigating brain oxygenation in acute stroke: Experience with a non-contrast quantitative BOLD based approach. Hum. Brain Mapp. 2853–2866. https://doi.org/10.1002/hbm.24564

Stone, A.J., Holland, N.C., Berman, A.J.L., Blockley, N.P., 2019b. Simulations of the effect of diffusion on asymmetric spin echo based quantitative BOLD: An investigation of the origin of deoxygenated blood volume overestimation. Neuroimage 201, 116035. https://doi.org/10.1016/j.neuroimage.2019.116035

Wharton, S., Bowtell, R., 2012. Fiber orientation-dependent white matter contrast in gradient echo MRI. Proc. Natl. Acad. Sci. 109, 18559–18564. https://doi.org/10.1073/pnas.1211075109

Wise, R.G., Harris, A.D., Stone, A.J., Murphy, K., 2013. Measurement of OEF and absolute CMRO2: MRI-based methods using interleaved and combined hypercapnia and hyperoxia. Neuroimage 83, 135–147. https://doi.org/10.1016/j.neuroimage.2013.06.008

Xu, F., Uh, J., Liu, P., Lu, H., 2012. On improving the speed and reliability of T 2-

relaxation-under- spin-tagging (TRUST) MRI. Magn. Reson. Med. 68, 198–204. https://doi.org/10.1002/mrm.23207

Yablonskiy, D.A., 1998. Quantitation of intrinsic magnetic susceptibility-related effects in a tissue matrix. Phantom study. Magn. Reson. Med. 39, 417–428. https://doi.org/10.1002/mrm.1910390312

Yablonskiy, D.A., Haacke, E.M., 1994. Theory of NMR Signal Behavior in Inhomogeneous Tissues: The Static. Magn. Reson. Med. 32, 749–763.

Yablonskiy, D.A., Sukstanskii, A.L., He, X., 2013. Blood oxygenation level-dependent (BOLD)-based techniques for the quantification of brain hemodynamic and metabolic properties - theoretical models and experimental approaches. NMR Biomed. 26, 963–986. https://doi.org/10.1002/nbm.2839

Zhang, Y., Brady, M., Smith, S., 2001. Segmentation of brain MR images through a hidden Markov random field model and the expectation-maximization algorithm. IEEE Trans. Med. Imaging. https://doi.org/10.1109/42.906424

Tables

Table 1: Parameter estimates of DBV and OEF calculated using sqBOLD, hqBOLD and TRUST. Median values in global grey matter are shown for each subject and presented alongside the group average, standard deviation and coefficient of variation.

Subject	Streamlined-qBOLD		Hyperoxia-qBOLD		TRUST
	DBV (%)	OEF (%)	DBV (%)	OEF (%)	OEF (%)
sub-01	1.6	10.0	1.3	49.6	38.7
sub-02	2.1	18.6	2.5	27.0	34.4
sub-03	4.7	12.5	1.4	56.6	34.1
sub-04	4.2	18.2	1.6	57.6	41.6
sub-05	2.5	9.7	1.5	30.6	27.5
sub-06	1.8	7.2	2.8	30.1	36.5
sub-07	4.5	15.8	1.2	54.6	53.3
sub-08	4.4	15.5	1.5	45.6	45.1
sub-09	4.4	9.2	1.1	40.1	48.6
sub-10	6.9	14.1	1.2	54.9	44.4
Mean	3.7	13.1	1.6	44.7	40.4
SD	1.7	4.0	0.6	11.9	7.7
CoV	0.45	0.30	0.36	0.27	0.19

Table 2: Regional estimates of $R_2'_{meas}$ and $R_2'_{sim}$. Median values in grey and white matter are shown for each subject and presented alongside the group average (± standard deviation). $R_2'_{sim}$ parameter maps were calculated from the combination of hyperoxia-BOLD DBV maps and global estimates of OEF made using TRUST (see Equation 6). $R_2'_{meas}$ parameter maps were measured using the FLAIR-GASE acquisition and acquired as part of the hqBOLD measurement of OEF.

Subject	**Grey Matter**		**White Matter**	
	$R_2'_{meas}$ (s^{-1})	**$R_2'_{sim}$ (s^{-1})**	**$R_2'_{meas}$ (s^{-1})**	**$R_2'_{sim}$ (s^{-1})**
sub-01	2.9	1.5	3.9	0.4
sub-02	2.2	2.6	3.0	0.9
sub-03	3.2	1.5	4.2	0.4
sub-04	3.5	2.0	4.7	0.7
sub-05	2.0	1.3	2.9	0.4
sub-06	2.8	3.1	3.6	1.1
sub-07	2.4	1.9	3.4	0.5
sub-08	2.8	2.1	3.9	0.5
sub-09	2.4	1.7	3.0	0.5
sub-10	4.3	1.6	5.8	0.4
Mean	2.8	1.9	3.8	0.6
SD	0.7	0.6	0.9	0.2
CoV	0.24	0.30	0.23	0.38

Figures

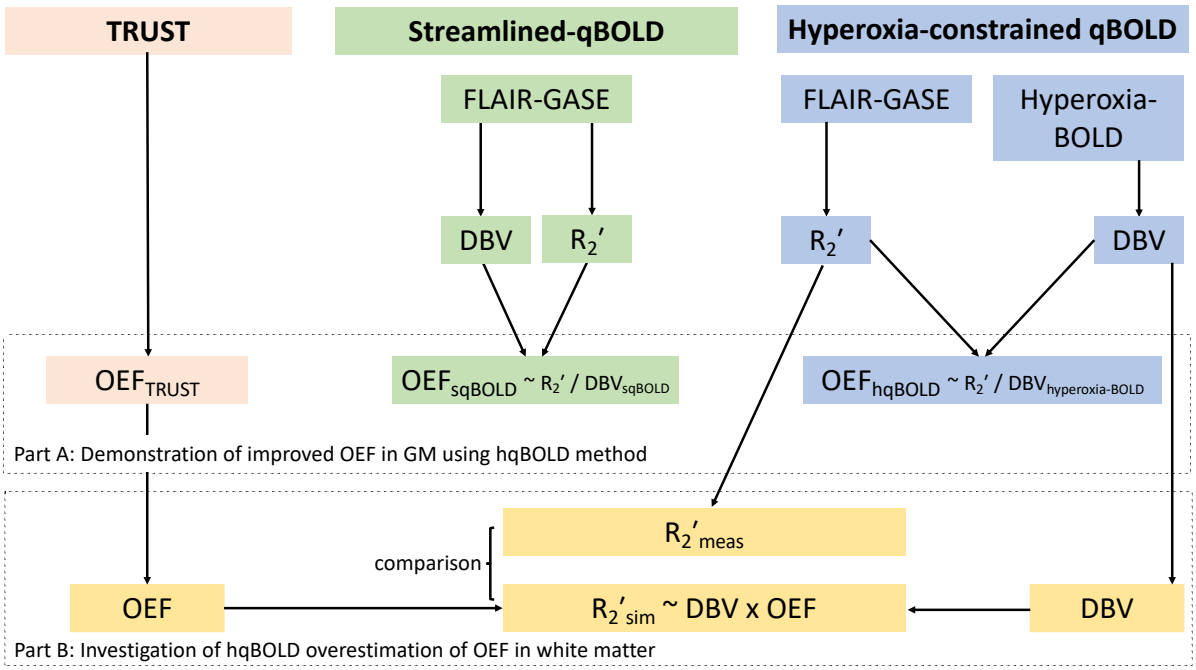

Figure 1: Schematic outlining the MR / physiological parameters derived from each imaging method. The first part of this study (Part A in schematic) focuses on demonstrating the improvement in grey matter OEF estimates that are achieved using the hqBOLD method. The second part of the study (Part B in schematic) investigates the origin of the OEF overestimation measured in white matter using hqBOLD.

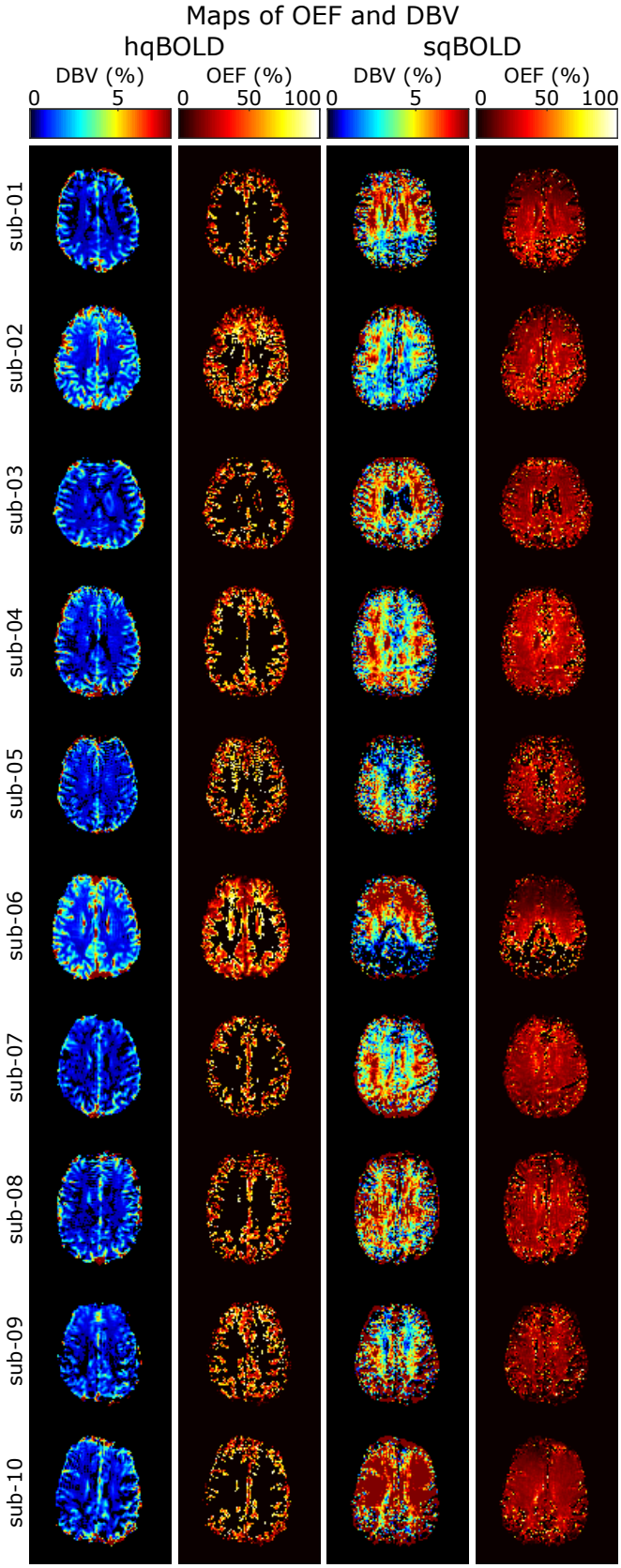

Figure 2: Individual parameter maps (single slice) produced using hqBOLD (DBV and OEF) and sqBOLD (DBV and OEF).

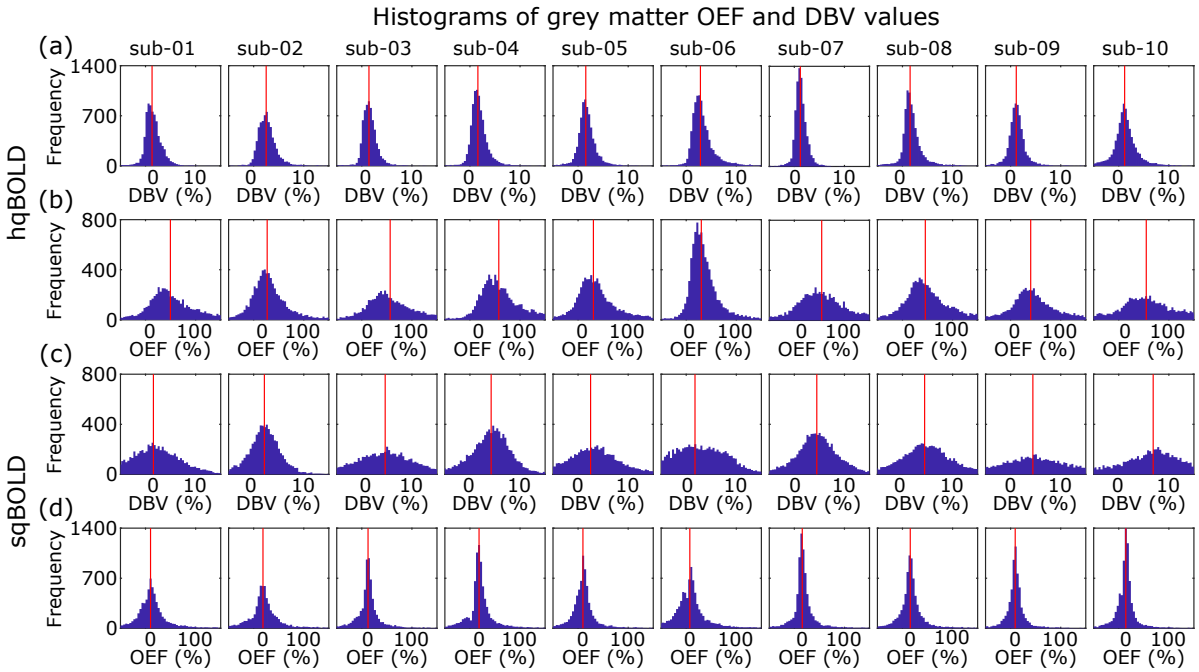

Figure 3: Histograms of DBV and OEF voxel values acquired using hqBOLD (a and b) and sqBOLD (c and d) restricted to the grey matter of each of the ten healthy subjects with the red line indicating the median.

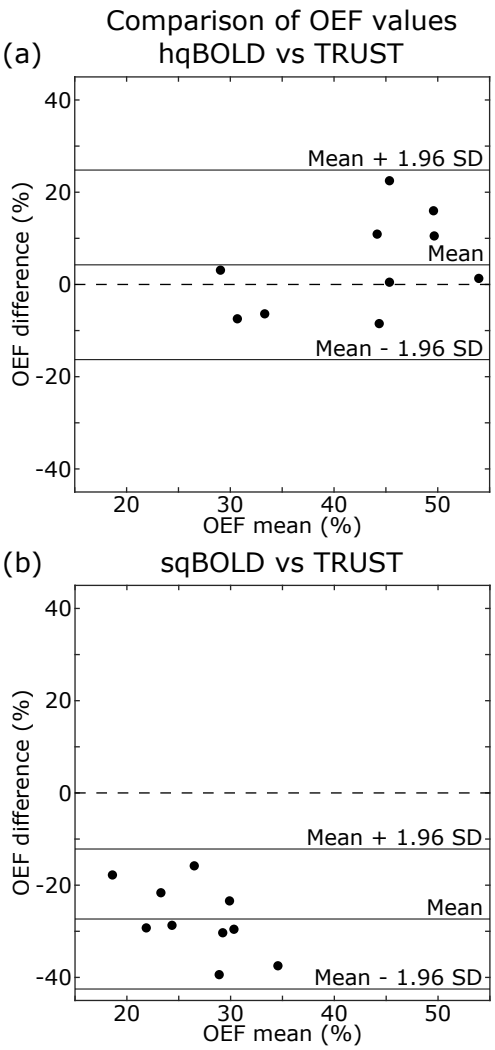

Figure 4: Bland-Altman plot comparing hqBOLD measures of OEF in global grey matter with sqBOLD and TRUST measures of OEF

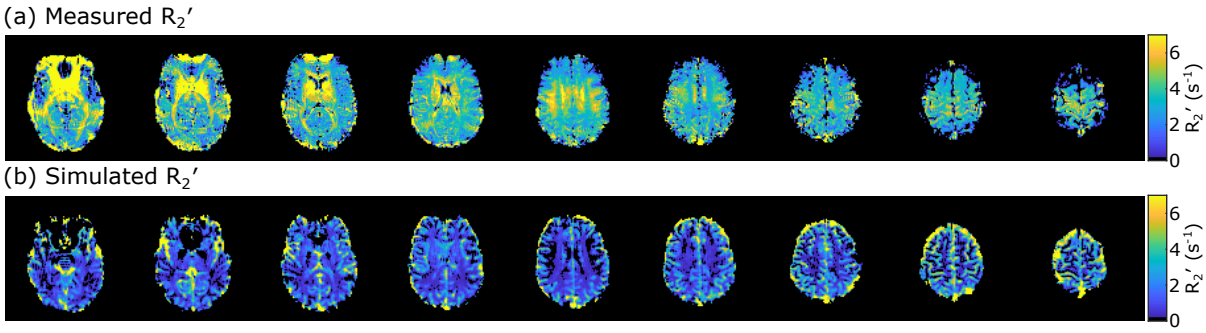

Figure 5: Comparison of parametric maps of $R_2'_{meas}$ and $R_2'_{sim}$ for a single subject.